Optical and X-Ray Studies of Indium Oxide Films Deposited by DC Magnetron Sputtering

A.A. Tikhii[a,*], E.A. Sviridova[b,c], Y.I. Zhikhareva[d,e] and I.V. Zhikharev[b]

[a] *Lugansk State Pedagogical University, Oboronnaya str., 2, 91011 Lugansk, Ukraine*
[b] *Donetsk Institute for Physics and Engineering named after A.A. Galkin, Rozy Lyuksemburg str. 72, 83114 Donetsk, Ukraine*
[c] *Donbas National Academy of Civil Engineering and Architecture, Derzhavina str. 2, 86123 Makeyevka, Ukraine*
[d] *Taras Shevchenko National University of Kyiv, Volodymyrska str. 64/13, 01601 Kyiv, Ukraine*
[e] *Institute of Industrial Economics of National academy of sciences of Ukraine, Maria Kapnist str. 2, 03057 Kyiv, Ukraine*

Received: 13.10.2023 & Accepted: 24.11.2023

Doi: 10.12693/APhysPolA.145.67 *e-mail: aatikhii@proton.me

The results of our studies on the structure and optical properties of In_2O_3 films deposited by DC magnetron sputtering onto Al_2O_3 (012) substrates are summarized. The films differ in terms of deposition time and substrate temperature. X-ray diffraction shows that the position and half-width of the peak related to the (222) plane of the cubic modification of In_2O_3 depends on the deposition time. Ellipsometric and optical transmission measurements show that the refractive index of films deposited on substrates at room temperature increases in the direction from the substrate to the external interface. The refractive index of the films deposited at a substrate temperature of more than 300°C is uniform, except for a rough layer on the surface. Annealing eliminates inhomogeneity of the refractive index and decreases the observed band gap for direct transitions. The latter results from a decrease in lattice defects concentration that causes a change in the Burstein–Moss shift. The true value of the band gap is insensitive to annealing.

topics: indium oxide films, band gap, optical properties, X-ray diffraction analysis

1. Introduction

In_2O_3 films have high optical transparency and good electrical conductivity, which is sensitive to gases, and doping enables obtaining a selective response [1–4]. Therefore, In_2O_3-based films are promising gas sensors. The rough surface is naturally formed during the growth of these films and makes them highly sensitive. The polycrystalline structure and strain also increase the sensitivity of such films by increasing the diffusion coefficients [5].

Quartz or passivated glass substrates are usually used to obtain polycrystalline indium oxide films. However, the use of sapphire substrates is justified by better thermal and chemical stability.

Most of the papers are devoted to epitaxial films on sapphire substrates [6–10], which, however, are rarely used for the deposition of polycrystalline films.

The method and modes of deposition have a substantial effect on the surface of the film [11]. The magnetron sputtering produces a higher surface roughness as compared to other methods [12]. In addition, this method is scalable and provides good performance and reproducibility of results. Also, it allows using a wide range of substrate temperatures during deposition [13, 14].

Ellipsometry and optical transmission are non-destructive optical research methods that allow non-contact measurement of the properties of nanoscale thin-film coatings. These methods complement each other as the influence of the material properties on ellipsometric measurements decreases with the distance to the surface, and there is no such dependence in the case of optical transmission.

In this paper, we summarize the results of our previous studies on the structure and optical properties of In_2O_3 films deposited onto Al_2O_3 (012) substrates in various modes of direct current (DC) magnetron sputtering [15–21].

2. Experiment

The films were deposited for 15–180 min at various substrate temperatures using the technique presented in the work [15]. After measurements, the deposited films were annealed in air for 1 h at 600°C and then studied again.

TABLE I

Characteristics of In_2O_3 films deposited at different substrate temperatures before annealing (deposition time — 1 hour).

T [°C]	Parameters of the film			Parameters of the rough layer			E_g^{Γ} [eV]	E_g^{indir} [eV]
	d [nm]	n	k	d [nm]	n	k		
Ellipsometric data [18–20]								
20	550	1.9 . . . 2	0	80	2 . . . 1.8	0		
300	450	2	0	75	2 . . . 1.53	0		
600	440	2.1	0	20	2.1 . . . 1.6	0		
Spectrophotometric data								
20	425	$0.81(n(\lambda)-1)$ $+1 \ldots n(\lambda)$	$0.81k(\lambda) \ldots k(\lambda)$	17	$n(\lambda) \ldots 0.5(n(\lambda)-1)+1$	$k(\lambda) \ldots 0.5k(\lambda)$	4.07	2.94
300	420	$n(\lambda)$	$k(\lambda)$	75	$n(\lambda) \ldots 0.1(n(\lambda)-1)+1$	$k(\lambda) \ldots 0.1k(\lambda)$	3.91	2.5
600	423	$n(\lambda)$	$k(\lambda)$	16	$n(\lambda) \ldots 0.75(n(\lambda)-1)+1$	$k(\lambda) \ldots 0.75k(\lambda)$	3.72	2.72

TABLE II

Characteristics of In_2O_3 films deposited at different substrate temperatures after annealing (deposition time — 1 hour).

T [°C]	Parameters of the film			Parameters of the rough layer			E_g^{Γ} [eV]	E_g^{indir} [eV]
	d [nm]	n	k	d [nm]	n	k		
Ellipsometric data [18–20]								
20	405	1.95	0	21	1.87 . . . 1.67	0		
300	450	2	0	20	1.8 . . . 1.5	0		
600	440	2.5	0	30	2 . . . 1.2	0		
Spectrophotometric data								
20	375	$n(\lambda)$	$k(\lambda)$	20	$n(\lambda) \ldots 0.75(n(\lambda)-1)+1$	$k(\lambda) \ldots 0.75k(\lambda)$	3.71	2.69
300	325	$n(\lambda)$	$k(\lambda)$	20	$n(\lambda) \ldots 0.75(n(\lambda)-1)+1$	$k(\lambda) \ldots 0.75k(\lambda)$	3.76	2.43
600	422	$n(\lambda)$	$k(\lambda)$	35	$n(\lambda) \ldots 0.75(n(\lambda)-1)+1$	$k(\lambda) \ldots 0.75k(\lambda)$	3.71	2.67

The ellipsometric measurements were carried out with a multi-angle null ellipsometer at a wavelength $\lambda = 632.8$ nm. The optical transmission was measured on a Shimadzu UV-2450 spectrophotometer. The composition of the targets and the films was analyzed using the X-ray diffractometer DRON-3.

3. Results and discussion

According to X-ray diffraction analysis, the studied films are polycrystalline and show a peak corresponding to the (222) plane of the cubic modification In_2O_3 (space group $Ia\bar{3}$) [16, 17].

Ellipsometric measurements [18–20] show an increase in the thickness d of the films with a decrease in the substrate temperature. The inhomogeneity of the films also increases with a decrease in the substrate temperature T. Thus, the refractive index n of films deposited on substrates at a temperature of 20°C increases linearly from 1.9 to 2 in the direction from the substrate to the rough layer (Table I). This may be caused by the increase in the surface temperature of the growing film during its deposition. Also, an increase in temperature leads to a decrease in surface roughness, which is modeled as a layer with a refractive index linearly decreasing in the direction of the environment. The initial and final values of the refractive index of the rough layer are also shown in Table I.

Annealing leads to the unification of the properties of the studied films and eliminates the inhomogeneity of the refractive index in the thickness direction (Table II) [18–20].

Now, we have confirmed these results based on the interference pattern observed in the spectrophotometric data (Fig. 1). The optical transmission spectra were calculated using the same models that were used for the processing of ellipsometric data. However, the spectral dependences of the refractive index $n(\lambda)$ and the extinction coefficient $k(\lambda)$ of the film material are taken according to [22]. The complex refractive indices of rough layers are calculated based on the refractive index of the film material by the Clausius–Mossotti equation. The calculated spectra are in reasonable agreement with the experimental results in the range of 500–1100 nm. The discrepancy between the calculated and experimental

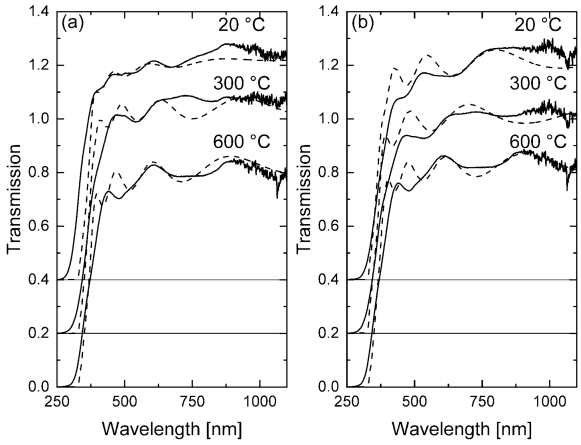

Fig. 1. Comparison of the calculated (dashed line) and measured optical transmission spectra (solid line) of the studied films before (a) and after annealing (b). The temperature of the substrate during the deposition process is shown in the graphs.

TABLE III

The thickness of the films with different deposition times (in nanometers) according to ellipsometric data [21].

Layer	Deposition time [min]				
	15	35	60	120	180
rough	26	25	25	22	25
In_2O_3	7	21	30	180	355
transition	20	11	6	7	6

values outside this region is due to the onset of fundamental absorption since the band gap of our films slightly differs from that of the films studied in [22]. (This material is characterized by a certain scatter in the values of the band gap depending on the production conditions according to [11]). The cause for the differences in the thicknesses of the layers found from ellipsometric measurements and measurements of optical transmission may be the different nature of the sensitivity of these methods, as well as the difference in the structure of real films from the proposed model. The latter is especially probable for the films obtained at room temperature. The greatest differences are in the estimates of the thickness of the surface layer since its optical properties are affected by the roughness profile, which is unknown for the samples under study.

The substrate temperature also affects the fundamental absorption edge of the films studied in [18–20]. The observed direct band gap E_g^{Γ} decreases with increasing temperature. The observed direct band gap also decreases as a result of annealing. This is well explained by the model of the band structure of In_2O_3 presented in the work [23]. According to this model, the observed direct band gap differs significantly from the real one due to the lattice symmetry and the Burstein–Moss shift. The latter significantly depends on defects in the crystal structure. The number of defects is smaller in films deposited on substrates with a higher temperature. Annealing in air eliminates oxygen vacancies. In turn, this reduces the concentration of charge carriers and the value of E_g^{Γ} [24, 25]. The band gap for "indirect" (forbidden by symmetry) transitions E_g^{indir} changes less due to electron–phonon interactions.

The structure of some of the investigated films deposited at a substrate temperature of 600°C depends on the deposition time [21]. Thus, according to the X-ray diffraction, the reflex corresponding to the (222) plane shifts from 30.3 to 30.6° with decreasing deposition time. The half-width of the reflex decreases in this case [17, 21].

The optical transmission of such films anomalously decreases with decreasing wavelength [21]. To describe their optical properties, we used a three-layer model. The first layer of this model describes the rough surface of the film as a homogeneous layer with optical properties calculated based on the dielectric constant of the cubic In_2O_3 modification and a fill factor of 0.5 using the Clausius–Mossotti equation. The optical properties of the second layer correspond to the cubic modification of In_2O_3 according to [22]. The third layer is characterized by a high extinction coefficient and is located between the film and the substrate. The spectrum of the extinction coefficient of this layer is fitted with the fundamental absorption of the semiconductor with $E_g^{\Gamma} = 1.39$ eV. According to ellipsometric measurements, its refractive index is close to 3. This agrees with the estimated refractive index of a semiconductor with a band gap of 1.39 eV, according to [26].

Table III shows that the thickness of the surface layer decreases and the thickness of the middle layer increases with increasing deposition time, while the total thickness of the film remains almost unchanged when the deposition time does not exceed 60 min. This suggests that films with a long deposition time contain, on average, smaller crystallites [17]. Thus, it can be assumed that large particles of the material are formed on the surface of the substrate when deposition begins, then the size of the resulting crystallites decreases during deposition, and they fill the gaps between larger particles. Later (60–180 min), the thickness of the surface layer is maintained when the total thickness of the film grows — the process of film formation reaches a stationary mode [21].

The transition layer at the interface with the substrate probably forms as a result of the presence of impurity levels inside the band gap and its smearing due to a large number of defects in the crystal structure. Since its thickness is practically independent of the deposition time, the appearance of this layer is completely due to the effect of the substrate surface.

4. Conclusions

The observed band gap of the studied films decreases with an increase in the substrate temperature during deposition. The annealing also decreases the observed band gap. This, as well as the differences in the refractive indices, thicknesses, and roughness of the films, is explained by the elimination of defects in the crystal structure under the influence of high temperatures in the presence of oxygen. The obtained values of the band gap agree with other studies [11, 22–25].

The optical properties of some In_2O_3 films indicate the presence of an additional layer with a band gap of 1.39 eV and a refractive index of 3 at the interface with the substrate. Also, during the growth of such films, the crystallite size changes, namely large particles of material are formed on the surface of the substrate at the beginning, then gaps between them are filled with smaller crystallites, and the process reaches a stationary mode.

References

[1] A.A. Yousif, M.H. Hasan, *J. Biosens. Bioelectron.* **6**, 1000192 (2015).

[2] J. Liu, W. Guo, F. Qu, C. Feng, C. Li, L. Zhu, J. Zhou, S. Ruan, W. Chen, *Ceram. Int.* **40**, 6685 (2014).

[3] A.A. Khalefa, J.M. Marei, H.A. Radwan, J.M. Rzaij, *Dig. J. Nanomater. Biostruct.* **16**, 197 (2021).

[4] D. Manno, M.D. Giulio, T. Siciliano, E. Filippo, A. Serra, *J. Phys. D Appl. Phys.* **34**, 2097 (2001).

[5] Yu.M. Nikolaenko, A.N. Artemov, Yu.Â. Medvedev, N.B. Efros, I.V. Zhikharev, I.Yu. Reshidova, A.A. Tikhii, S.V. Kara-Murza, *J. Phys. D Appl. Phys.* **49**, 375302 (2016).

[6] S. Kaneko, H. Torii, M. Soga, K. Akiyama, M. Iwaya, M. Yoshimoto, T. Amazawa, *Jpn. J. Appl. Phys.* **51**, 01AC02 (2012).

[7] S.K. Yadav, S. Das, N. Prasad, B.K. Barick, S. Arora, D.S. Sutar, S. Dhar, *J. Vac. Sci. Technol. A* **38**, 033414 (2020).

[8] X. Du, J. Yu, X. Xiu, Q. Sun, W. Tang, B. Man, *Vacuum* **167**, 1 (2019).

[9] M. Nistor, W. Seiler, C. Hebert, E. Matei, J. Perrière, *Appl. Surf. Sci.* **307**, 455 (2014).

[10] W. Seiler, M. Nistor, C. Hebert, J. Perrière, *Solar Energy Mater. Solar Cells* **116**, 34 (2013).

[11] M.Z. Jarzebski, *Phys. Stat. Sol. (a)* **71**, 13 (1982).

[12] H. Kim, C.M. Gilmore, A. Pique, J.S. Horwitz, H. Mattoussi, H. Murata, Z.H. Kafafi, D.B. Chrisey, *J. Appl. Phys.* **86**, 6451 (1999).

[13] M. Higuchi, S. Uekusa, R. Nakano, K. Yokogawa, *J. Appl. Phys.* **74**, 6710 (1993).

[14] Y. Shigesato, S. Takaki, T. Haranoh, *J. Appl. Phys.* **71**, 3356 (1992).

[15] Yu.M. Nikolaenko, A.B. Mukhin, V.A. Chaika, V.V. Burkhovetskii, *Tech. Phys.* **55**, 1189 (2010).

[16] A.A. Tikhii, Yu.M. Nikolaenko, Yu.I. Zhikhareva, I.V. Zhikharev, in: *7th Int. Congress on Energy Fluxes and Radiation Effects (EFRE-2020 online): Abstracts*, Publishing House of IAO SB RAS, Tomsk, Russia 2020 p. 601.

[17] A.A. Tikhii, Yu.M. Nikolaenko, Yu.I. Zhikhareva, I.V. Zhikharev, *Opt. Spectr.* **128**, 1667 (2020).

[18] A.A. Tikhii, Yu.M. Nikolaenko, Yu.I. Zhikhareva, A.S. Kornievets, I.V. Zhikharev, *Semiconductors* **52**, 320 (2018).

[19] V.A. Gritskikh, I.V. Zhikharev, S.V. Kara-Murza, N.V. Korchikova, T.V. Krasnyakova, Y.M. Nikolaenko, A.A. Tikhii, A.V. Pavlenko, Y.I. Yurasov, in: *Advanced Materials Techniques, Physics, Mechanics and Applications* Eds: I.A. Parinov, S.-H. Chang, M.A. Jani, *Springer Proceedings in Physics*, Vol. 193, Springer International Publishing AG., 2017, p. 55.

[20] A.A. Tikhii, V.A. Gritskikh, S.V. Kara-Murza, N.V. Korchikova, Yu.M. Nikolaenko, Yu.I. Zhikhareva, I.V. Zhikharev, in: *European Materials Research Society Spring Meeting 2016 (E-MRS 2016)*, Lille (France) 2023, L.P.32.

[21] A.A. Tikhii, K.A. Svyrydova, Yu.I. Zhikhareva, I.V. Zhikharev, *J. Appl. Spectr.* **88**, 975 (2021).

[22] A. Schleife, M.D. Neumann, N. Esser, Z. Galazka, A. Gottwald, J. Nixdorf, R. Goldhahn, M. Feneberg, *New J. Phys.* **20**, 053016 (2018).

[23] A. Walsh, J.L.F. Da Silva, S.-H. Wei et al., *Phys. Rev. Lett.* **100**, 167402 (2008).

[24] Y. Furubayashi, M. Maehara, T. Yamamoto, *ACS Appl. Electron. Mater.* **1**, 1545 (2019).

[25] L. Gupta, A. Mansingh, P.K. Srivastava, *Thin Solid Films* **176**, 33 (1989).

[26] N.M. Ravindra, P. Ganapathy, J. Choi, *Infrared Phys. Technol.* **50**, 21 (2007).